Nuclear Instruments and Methods in Physics Research B xxx (2017) xxx–xxx

Contents lists available at ScienceDirect

Nuclear Instruments and Methods in Physics Research B

journal homepage: www.elsevier.com/locate/nimb

Accelerator Mass Spectrometry on SIRIUS: New 6 MV spectrometer at ANSTO

K.M. Wilcken [a,*], D. Fink [a], M.A.C. Hotchkis [a], D. Garton [a], D. Button [a], M. Mann [a], R. Kitchen [b], T. Hauser [b], A. O'Connor [b]

[a] Australian Nuclear Science & Technology Organisation, Sydney, New South Wales, Australia
[b] National Electrostatics Corporation, 7540 Graber Road, Middleton, WI 53562-0310, United States

ARTICLE INFO

Article history:
Received 5 August 2016
Received in revised form 23 December 2016
Accepted 4 January 2017
Available online xxxx

Keywords:
Accelerator Mass Spectrometry
Cosmogenic isotopes
^{10}Be
^{26}Al
^{36}Cl

ABSTRACT

The Centre for Accelerator Science at ANSTO operates four tandem accelerator systems for Accelerator Mass Spectrometry (AMS) and Ion Beam Analysis (IBA). The latest addition to the fleet is SIRIUS, a 6 MV combined IBA and AMS system. Following initial ion beam testing, conditioning and debugging software and hardware, SIRIUS is now commissioned. Details of the instrument design and performance data for ^{10}Be, ^{26}Al and ^{36}Cl are presented.

© 2017 Elsevier B.V. All rights reserved.

1. Introduction

In 2009, the Australian Federal Government, under its Educational Investment Fund, funded the establishment of the Centre for Accelerator Science at ANSTO. Funds were made available to purchase two new tandem accelerator systems, an accelerator hall, and a comprehensive suite of geochemistry laboratories for AMS sample processing for ^{10}Be, ^{26}Al, ^{36}Cl and actinides. The 1 MV instrument, VEGA, dedicated for AMS with radiocarbon and actinides [1] is in routine operation. The larger 6 MV pelletron accelerator from NEC, SIRIUS, is presented here in terms of its AMS performance for cosmogenic isotopes ^{26}Al, ^{10}Be and ^{36}Cl. The aspects of the Ion Beam Analysis functionality were previously reported in [3]. Given we host a range of accelerators our focus with SIRIUS regarding AMS will be on cosmogenic isotopes and the older instrument ANTARES [2] will be directed away from routine analysis towards particular applications where the highest ion energies are required.

2. Spectrometer

2.1. Layout

The layout of the spectrometer is shown in Fig. 1. The ion source is a 134 sample MC-SNICS at 100 keV maximum beam energy (10 kV sputter voltage, 20 kV ion extraction and 70 kV source bias) that incorporates essential design concepts from earlier studies [4,5] to improve vacuum and to reduce beam emittance. The key difference to earlier MC-SNICS version is in extractor lens geometry and pre-acceleration section which have been replaced with a gap lens. The low energy injector section of the spectrometer comprises a rotatable 45° spherical electrostatic analyser (R = 0.3 m, d = 40 mm with an option for a second ion source) and a 90° high resolution double focusing magnet, MEP = 20 amu MeV, 70 mm vacuum gap, with central trajectory radius of 1 m. Mass resolution $M/\Delta M$ of the magnet was specified to be at least 500 which has been experimentally verified. The magnet chamber is electrically insulated allowing fast switching between isotopes with maximum +15 kV bounce voltage. The switching time with the large magnet chamber per 10 kV change is about 100 μs. Typical sequence during, for example beryllium measurement is 0.3 ms for ^{9}Be and about 100 ms for ^{10}Be with 100 μs waiting times between isotopes resulting in a bouncing frequency of about 10 Hz. No separate blanking steerer is used during switching between isotopes.

An electrostatic triplet lens at the entry to the accelerator, coupled with a 2/3 reduction in voltage gradient across the first 6 acceleration gaps is used to achieve beam focus at the stripper canal (930 mm long with a constant diameter of 11.5 mm) in the terminal. The stripper is differentially pumped with two recirculating turbo pumps and there is a choice of two gases, currently He and Ar, installed in the terminal. The base vacuum at the entry and exit of the accelerator is 2×10^{-6} Pa and 4×10^{-6} Pa,

* Corresponding author.
E-mail address: klaus.wilcken@ansto.gov.au (K.M. Wilcken).

http://dx.doi.org/10.1016/j.nimb.2017.01.003
0168-583X/© 2017 Elsevier B.V. All rights reserved.

Please cite this article in press as: K.M. Wilcken et al., Accelerator Mass Spectrometry on SIRIUS: New 6 MV spectrometer at ANSTO, Nucl. Instr. Meth. B (2017), http://dx.doi.org/10.1016/j.nimb.2017.01.003

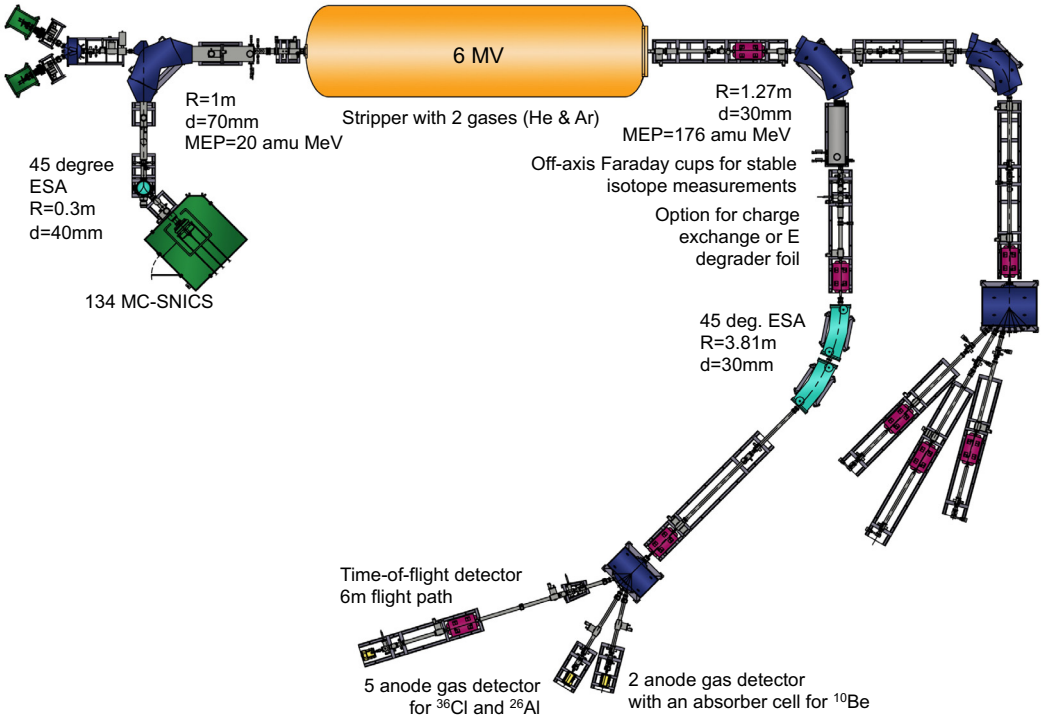


Fig. 1. Schematic layout of SIRIUS - ANSTO's new 6 MV accelerator system (note: TOF beam-line is at +14° and not as shown in schematic).

respectively, when the metering valve that controls the stripper gas (Ar) is closed. This increases to about 1.4×10^{-5} Pa both at entry and exit of the accelerator at typical ^{10}Be operating conditions using argon. Beam-line vacuum is measured with hot-cathode Bayard–Alpert ionization vacuum gauges. Accelerator voltage is applied via a pelletron charging system and GVM terminal voltage stabilisation with corona feedback is used for AMS. Alternatively for IBA operation, slit stabilisation using high energy slits after the IBA analyser magnet is also possible.

At the high energy end an in-tank electrostatic quadrupole triplet focuses the beam to the object point of the 90° double focusing analysing magnet with MEP = 176 amu MeV, central trajectory radius of 1.27 m and vacuum gap of 30 mm. At the magnet image focal position there are 3 off-axis Faraday cups for stable isotope measurements, one at the high mass side and two at the low mass side. Beam width (FWHM) at the analyser magnet image position for $^{13}C^{4+}$ beam at 5.4 MV terminal voltage and Ar stripper gas is about 1 mm. Immediately following the analyser magnet image Faraday cup, a multiple position actuator assembly provides an option to insert various foils for energy degrading or charge-exchange foil for enhanced isobar suppression. Energy filtering to reject tails from adjacent isotope masses is provided by a 45° spherical electrostatic analyser (made up from a coupled 22.5° pair) with central trajectory radius of 3.81 m, plate separation of 30 mm and maximum E/Q of 7.6. After the energy analyser, a switching magnet with a vacuum gap of 30 mm transports the beam to one of 3 AMS beam lines each with its own dedicated AMS detector setup through bending angles of ±14° (MEP = 693 amu MeV) or −28° (MEP = 176 amu MeV), depending on which rare isotope species is being measured. The exit ports at ±45° (MEP = 70 amu MeV) and at +28° are not currently used. The high energy AMS section is equipped with two magnetic quadrupoles triplets – the first lens before the spherical ESA is for image correction and the second lens before the switching magnet focus the beam to the detectors at the end of each AMS beam line. For the time-of-flight detector there is an additional quadrupole between the start and stop detectors for increased transmission efficiency [6].

2.2. Ion detection & data acquisition

The beam line at −28° is dedicated for ^{10}Be and has an absorber cell permanently assembled in front of the 2-anode gas ionisation detector. The absorber cell and detector design follows very closely an earlier design reported by [7] but with only the first two anodes in use. Effective suppression of ^{10}B during ^{10}Be measurement is achieved with 5 μm thick Havar window and 9.4 kPa of Ar for the absorber cell followed by 5 μm thick Mylar and 4.0 kPa isobutane for the detector. The length of the absorber cell and active detector volume are 190 and 240 mm, respectively.

For ^{36}Cl and ^{26}Al measurements we use a second beam line (−14° exit port) with a multipurpose 5-anode gas ionisation detector that is very similar to the one presented in detail earlier [7,8]. The entrance window to the detector (SiN membrane that is currently 50 nm thick and 10 mm by 10 mm in size) is mounted on an insulating holder that positions the window under the dE_1 anode plate. Peak resolutions based on ^{36}Cl data from the first two anode plates, dE_1 and dE_2, are very similar indicating that the electron collection on dE_1 is not compromised due to electric field line distortions at the entry to the detector. Energy signals are collected by ORTEC 142PC or Amptek A250CF pre-amplifiers; at the typical 0.5–1 range in MeV/amu we see little or no difference in performance.

Detector signals are digitised with customised XIA's DGF-Pixie-4 cards offering a maximum of 16 channels of data when using all 4 units in parallel. In practice not all the channels are used at once but are shared between detector stations offering back-up modules in case of failures and avoiding the need to switch cables when operating different detectors. The signal digitisation can be done

Please cite this article in press as: K.M. Wilcken et al., Accelerator Mass Spectrometry on SIRIUS: New 6 MV spectrometer at ANSTO, Nucl. Instr. Meth. B (2017), http://dx.doi.org/10.1016/j.nimb.2017.01.003

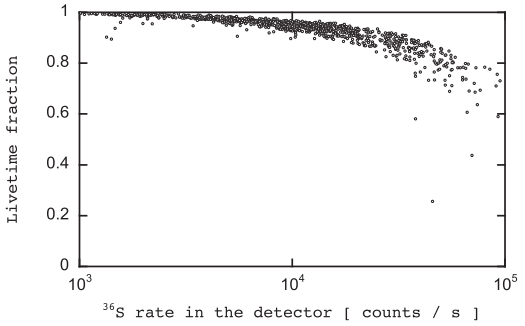


Fig. 2. Livetime fraction presented as a function of gross ^{36}S rate in the detector when the rate seen by the Pixie interface and data acquisition computer was a factor of 10 lower followed by the single-channel analysis as discussed in the text.

in two different modes either by operating the DGF-Pixie-4 cards as fast and continuous pulse digitisers where pulse shaping for amplitude detection is performed in software using the tail pulses directly from the preamplifiers as inputs, or as conventional peak-sensing ADCs when the pre-amplifier signal is instead first shaped (in hardware) with regular analog linear amplifiers such as ORTEC 570s before signal digitisation in the Pixie-4 cards using a peak-sensing algorithm. In our previous work on the 1 MV VEGA accelerator at far lower ion energies [1] we opted for the latter due to concerns regarding the signal resolution when a large part of the ADC voltage range was taken up by baseline fluctuations and potential distortions in the shape of the peaks. With higher ion energies, the signal to noise ratio is improved but the preference is still to operate the system in the peak-sensing mode with analog amplifiers. The two major reasons for this are the familiar and established performance, and the option to heavily reduce the count rate from interfering ions with a single-channel analyser thus avoiding potential issues of overfilling the buffer memory.

In this mode the system can sustain count rates up to about 20 k events per second in the detector before significant distortions in peak shape and position appear. Detector and data acquisition dead time is measured with a regular pulser technique where a pulse generator at about 20 Hz is fed through the detector electronics, integrated in the spectra and then compared to an independent fast scaler fed by the same pulser. The livetime of the detector and data acquisition is shown in Fig. 2 as a function of ^{36}S rate in the detector: the data were acquired with the system setup for ^{36}Cl measurement and the high rate of ^{36}S incident on the detector was reduced by factor of 10 with a single-channel analyser before feeding the pulses into the Pixie-4 cards.

3. AMS performance

3.1. ^{26}Al

AMS measurement of cosmogenic ^{26}Al is usually simpler than other isotopes as the isobar ^{26}Mg does not form a stable negative ion and can be avoided by selecting elemental negative ion injection for analysis. However, negative ion yields for Al are low and counting statistics often limits the achievable measurement precision. Measured particle transmission through the accelerator from injected Al^- to analysed Al^{3+} at the high energy end is 40% with Ar stripper gas. The measured ^{26}Al/^{27}Al ratios of standard reference materials are about 90% from the nominal value. The distribution of unnormalised (raw) primary standard measurements during an AMS run of 5 days is shown in Fig. 3 (for KN-4-2) and has an average of $(2.716 \pm 0.024) \times 10^{-11}$. For background samples the measured ^{26}Al/^{27}Al ratios are typically below 1×10^{-15} but due

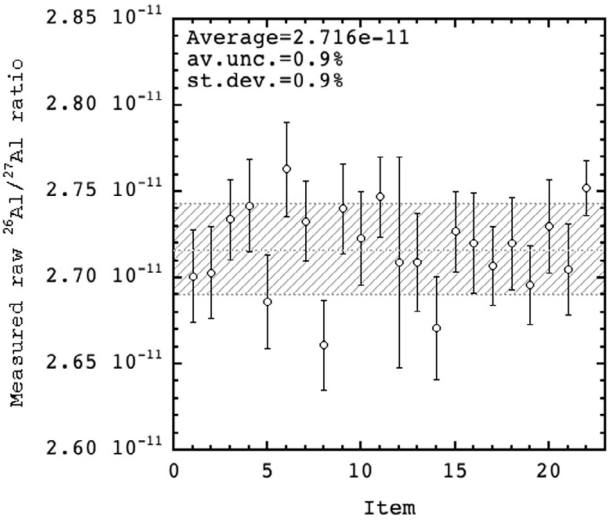


Fig. 3. Measured raw ratios of Al primary standard KN-4-2 with nominal value of 3.096×10^{-11} [9] plotted as a function of run order over 5 days. Each data point represents the linear average of at least three repeat measurements (usually 3 or 4) on a single cathode. The data has no trend or additional random error beyond the measurement uncertainty $\sim 1\%$ that is assigned to be either counting statistics or standard deviation of the mean whichever is larger.

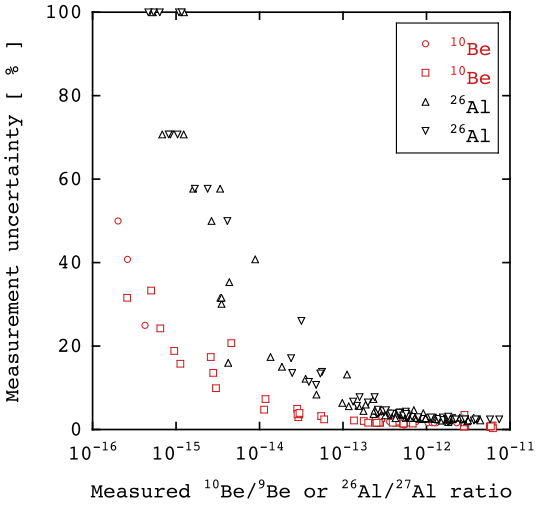


Fig. 4. Typical measurement uncertainty for a suite of ^{10}Be (in red) and ^{26}Al (in black) samples with varying rare isotope ratios from very high (1×10^{-11}) to blanks $\sim 5 \times 10^{-16}$). The different symbols per radioisotope denote data from two independent experiments. Each data point represents the average ratio of repeats based on an algorithm that ceases further measurement once a 2–3% statistical precision has been achieved and at least 3 repeats completed. This constraint results in high ratio samples being measured to completion sooner and low ratio samples requiring sputtering of up to 48 min (i.e. 8 repeats with each lasting 6 min). Longer sputtering times will improve precision for low ratio samples until the limit of system efficiency is reached. (For interpretation of the references to colours in this figure legend, the reader is referred to the web version of this paper.)

to low counting statistics the measurement have large errors, see Fig. 4.

Typically $^{27}Al^-$ currents from our ion source are in the range from 300 to 800 nA. This may not be optimal in terms of ion source efficiency or negative ion output but at these early stages of our spectrometer's operation, we prefer stable reliable operation over maximum performance. Currently, the practical ionisation efficiency for Al^- in our source is 0.13%, measured by comparing the total ^{26}Al counts in the detector to the calculated inventory of ^{26}Al inserted in the cathode (based on Al oxide mass and isotopic

Please cite this article in press as: K.M. Wilcken et al., Accelerator Mass Spectrometry on SIRIUS: New 6 MV spectrometer at ANSTO, Nucl. Instr. Meth. B (2017), http://dx.doi.org/10.1016/j.nimb.2017.01.003

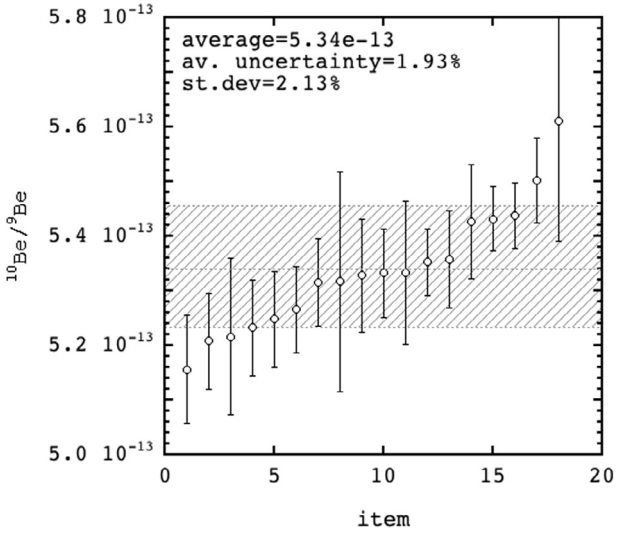


Fig. 5. Collected results from two AMS runs for KN-6-2 standard material (nominal value 5.349×10^{-13}) normalised to primary standard KN-5-4 (nominal value 2.851×10^{-12}) [11]. The average measurement error is 1.9% and a population (n = 18) standard deviation of 2.1%.

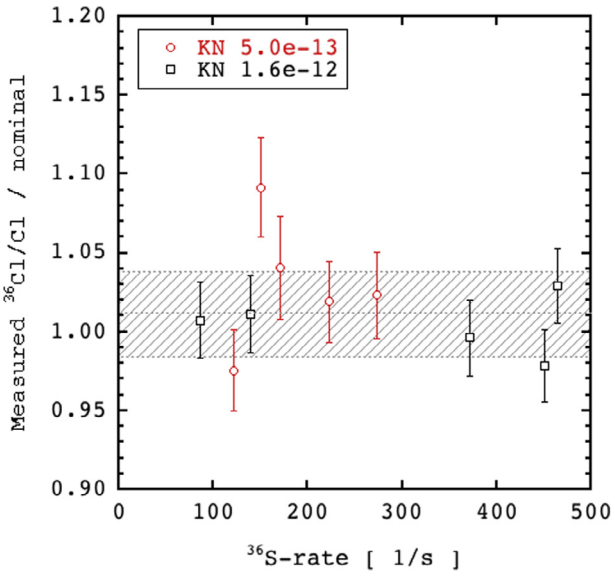


Fig. 6. Measured ^{36}Cl/Cl ratios from KN 1.600×10^{-12} and 5.00×10^{-13} materials [13] normalised to their respective nominal value and plotted against ^{36}S-rate. Weighted average of the measurements 1.011 ± 0.026 is consistent with the nominal value.

Table 1
Detector resolutions during ^{36}Cl measurement and figure-of-merit (FOM) values for each channel of data.

Signal	Resolution [%]	FOM
dE_1	3.8	2
dE_2	3.7	0.6
$dE_{3A\&B}$	14.5	n.a.
dE_4	6.7	2
dE_5	18.8	2.6
E_{TOT}	0.7	n.a.

ratio) when run to exhaustion and after correcting for transmission and normalisation factors. Typical ranges in measurement uncertainty for a collection of routine samples is shown in Fig. 4 as a function of the ^{26}Al/^{27}Al ratio. Given the demonstrated ~1% reproducibility for primary standards in Fig. 3 and low ion source output it follows that the measurement uncertainty for unknown samples is typically dominated by counting statistics.

3.2. ^{10}Be

For our ^{10}Be measurements we extract typically 8–15 μA of BeO^- from the ion source. Measured particle transmission through the accelerator from the injected BeO^- to analysed Be^{3+} at the high energy end is about 35% at 6 MV terminal voltage with Ar stripper gas. The interfering ^{10}B isobar is suppressed with a passive absorber cell in front of the gas ionisation detector and the measured ^{10}Be/^{9}Be ratios are about 80% of the nominal values. We have chosen not to use an energy degrader foil technique [10] to suppress ^{10}B as this inevitably reduces the overall efficiency of the measurement. Typical measurement uncertainties as a function of ^{10}Be/^{9}Be ratio are shown in Fig. 4 together with similar data for ^{26}Al. Given the higher ion source output it is clear that one reaches better precision with ^{10}Be for lower ratio samples than with ^{26}Al.

For our lowest ^{9}Be-carrier prepared from a phenakite solution with minimal sample processing (ie. directly calcined without initial conversion to Be hydroxide), measured ^{10}Be/^{9}Be ratios fall in the range of $(2–6)\times10^{-16}$. The ^{10}Be/^{9}Be ratio from the same phenakite carrier following full chemistry processing as per our methods for quartz samples, results in a ratio of about 1×10^{-15}. Measurement uncertainty at these very low levels range from 20% to 50%, as shown in Fig. 4.

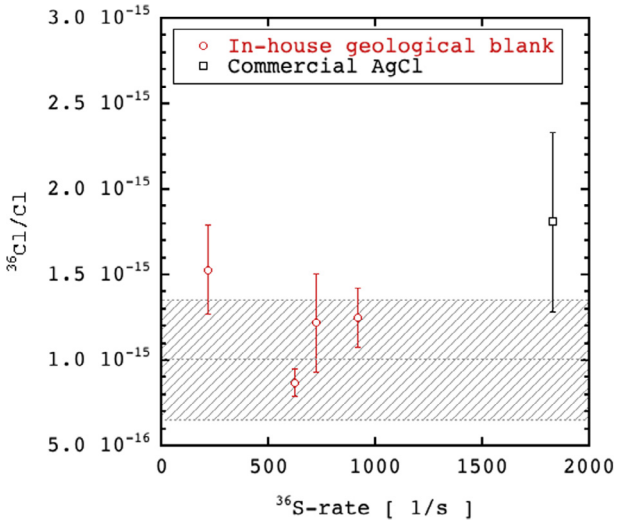


Fig. 7. A set of blank samples presented as a function of the ^{36}S-rate. The weighted average of the 5 samples including geological background material and commercial AgCl is $(1.01 \pm 0.35 \times 10^{-15})$.

To complement the presentation of (raw) unnormalised results for ^{26}Al in Fig. 3, a compilation of results for ^{10}Be standard material KN-6-2 (nominal value 5.349×10^{-13} [11]) that was measured as secondary standard in two separate AMS runs is shown in Fig. 5. The measurements were normalised using KN-5-4 (nominal value 2.851×10^{-12}) as primary standard. Given the far higher ion source yields for BeO^- compared to Al^- we were able to use a reference standard with a factor of 100 lower ratio that better mimics the typical unknown sample. Also using secondary standards allows inclusion of errors in the normalisation into our assessment. The average value of the 18 measurements, $5.34 \pm 0.11 \times 10^{-13}$ is identical to the nominal value within the measurement uncertainty. Samples were run using the same algorithm as for ^{26}Al requiring at least 3 repeats per target and a total statistical uncertainty of at most 2% for each target.

Please cite this article in press as: K.M. Wilcken et al., Accelerator Mass Spectrometry on SIRIUS: New 6 MV spectrometer at ANSTO, Nucl. Instr. Meth. B (2017), http://dx.doi.org/10.1016/j.nimb.2017.01.003

Table 2
Summary of the key performance data for AMS measurements of ^{10}Be, ^{26}Al and ^{36}Cl. Normalisation factor is defined as the measured ratio divided by the nominal value. Measurement uncertainty σ is defined from distribution of results for standard materials at 1×10^{-12} to 1×10^{-11} level as discussed in the text.

Species	Ion source		Accelerator				Performance	
	Output [μA]	Efficiency [%]	TV	q	Transmission [%]	Norm.factor	Background	σ [%]
^{10}Be	8–15	n.a.	6.0	3	35	1.25	2e−16	2
^{26}Al	0.3–0.8	0.13	4.0	3	40	1.15	<1e−15	1
^{36}Cl	10–20	n.a.	6.0	5	25	~2	~1e−15	3

3.3. ^{36}Cl

Given Cl is a prolific negative ion it is very easy to produce high output from the source as compared to aluminium or even beryllium. However, in practice the source output is typically kept at moderate levels to avoid potential challenges in beam transport, ion source memory and increasing ^{36}S rate in the detector. The challenge with ^{36}Cl measurements is to reduce the absolute ^{36}S isobar rate sufficiently to a level which will allow unambiguous identification of ^{36}Cl events for samples with ^{36}Cl/Cl ratios in the 1×10^{-15} range. This requirement places stringent demands on sample processing, optimising detector energy resolutions, reducing scattered ^{36}S events and enhancing peak-to-peak ^{36}S to ^{36}Cl separations in the multi-anode gas ionisation detector. In general the higher the ion energy the better the separation between ^{36}Cl and ^{36}S is, see for example [6]. However it has been shown that ion energies around 30 MeV are sufficient for efficient measurement of ^{36}Cl [8,12].

For our ^{36}Cl measurement we extract 10–20 μA beams of ^{35}Cl$^-$ from the source, and select 5+ ions for analysis. With 6 MV terminal voltage and Ar gas stripper, transmission to the detector Faraday cup for 5+ is about 25%. For ^{36}Cl ion counting we use 5 active anode delta-E signals and a (diagonally) split dE_3 signal in the gas ionisation detector. A total energy signal is also available and used for diagnostic purposes. The peak resolutions and figure-of-merit, defined as difference in the ^{36}Cl − ^{36}S peak positions divided by the average full width at half maximum, are given in Table 1. As was found in the earlier works [8,12] it is important to reduce the impact of scattered ^{36}S ions that might appear as fictitious ^{36}Cl signal which would limit the achieved suppression factor between ^{36}S and ^{36}Cl, we do this with the split dE_3 anodes.

Collection of secondary standard measurements from KN 1.600×10^{-12} and KN 5.00×10^{-13} materials [13] are shown in Fig. 6. The measurements were normalised to Purdue Z93-0005 primary standard with nominal value of 1.200×10^{-12}. The normalised measured values for these two secondary standards are $(1.607\pm0.030)\times10^{-12}$ and $(5.12\pm0.21)\times10^{-13}$, respectively, with n = 5. The ^{36}S-rate from the standards was below 500 counts per second whilst ^{35}Cl$^-$ current was typically around 20 μA allowing simple and reproducible measurements.

To demonstrate the capability of the system a collection of results from two background samples (4 targets from a geological mineral and one target from commercial AgCl) are shown in Fig. 7 as a function of their average ^{36}S-rate, which ranged from a few hundred counts to about 2000 counts per second. The weighted average of the 5 samples is $1.01\pm0.35\times10^{-15}$. With our limited dataset we are not yet able to characterise the dependency of these background measurements on the ^{36}S-rate.

4. Conclusions

The new 6 MV spectrometer SIRIUS has successfully been commissioned and measurement methods for ^{10}Be, ^{26}Al and ^{36}Cl samples have been established. The key performace data are summarised in Table 2. We expect to implement gradual improvements for each isotope over time but the achieved performance is already sufficient for most applications utilising cosmogenic isotopes.

Our older spectrometer ANTARES [14] is currently not setup for ^{36}Cl measurements and although reproducibility for ^{10}Be is a good ~2% at 1×10^{-11} level, background ^{10}Be/Be results are limited to $(2–5)\times10^{-15}$ even with our lowest ^{9}Be phenakite carrier resulting mainly from poor beam-line vacuum and a restricted high-energy analyser. Similarly for ^{26}Al, the reproducibility with ANTARES is (2–3)% for 1×10^{-11} level samples and background is an acceptable 2×10^{-15}, the ion-source output is rarely above 400 nA. For both ^{10}Be^{3+} and ^{26}Al^{5+} ANTARES measurements, transmission have been increased from 32% and 25% to about 35% for ^{10}Be^{3+} and 40% for ^{26}Al^{3+} on SIRIUS, respectively. Therefore even at these early stages the performance of the new bespoke spectrometer is providing a significant upgrade on the larger legacy accelerator system ANTARES via specifically lower backgrounds and slightly better reproducibility but with the added convenience of unattended operation.

Acknowledgements

We acknowledge Australian Federal Government support through the Educational Investment Fund that provided infrastructure funding to establish the Centre for Accelerator Science at ANSTO and also the National Collaborative Research Infrastructure Strategy (NCRIS) which provides partial funding for operations of Centre for Accelerator Science.

References

[1] K.M. Wilcken, M. Hotchkis, V. Levchenko, D. Fink, T. Hauser, R. Kitchen, Nucl. Instrum. Methods Phys. Res. B 361 (2015) 133–138.
[2] D. Fink, M. Hotchkis, Q. Hua, G. Jacobsen, A.M. Smith, U. Zoppi, D. Child, C. Mifsud, H. van der Gaast, A. Williams, M. Williams, Nucl. Instrum. Methods Phys. Res. B 223–224 (2004) 109–115.
[3] Z. Pastuovic, D. Button, D. Cohen, D. Fink, D. Garton, M. Hotchkis, M. Ionescu, S. Long, V. Levchenko, M. Mann, R. Siegele, A. Smith, K. Wilcken, Nucl. Instrum. Methods Phys. Res. B 371 (2016) 142–147.
[4] J.R. Southon, G.M. Santos, Radiocarbon 46 (1) (2004) 33–39.
[5] J.R. Southon, G.M. Santos, Nucl. Instrum. Methods Phys. Res. B 259 (2007) 88–93.
[6] L.K. Fifield, S.G. Tims, J.O. Stone, D.C. Argento, M. De Cesare, Nucl. Instrum. Methods Phys. Res. B 294 (2013) 126–131.
[7] C. Maden, P.A.F. Anastasi, A. Dougans, S.P.H.T. Freeman, R. Kitchen, G. Klody, C. Schnabel, M. Sundquist, K. Vanner, S. Xu, Nucl. Nucl. Instrum. Methods Phys. Res. B 259 (2007) 131–139.
[8] K.M. Wilcken, S.P.H.T. Freeman, A. Dougans, S. Xu, R. Loger, C. Schnabel, Nucl. Instrum. Methods Phys. Res. B 268 (2010) 748–751.
[9] Kunihiko Nishiizumi, Nucl. Instrum. Methods Phys. Res. B 223–224 (2004) 388–392.
[10] E. Nottoli, M. Arnold, G. Aumaître, D.L. Bourlès, K. Keddadouche, M. Suter, Nucl. Instrum. Methods Phys. Res. B 294 (2013) 397–402.
[11] K. Nishiizumi, M. Imamura, M.W. Caffee, J.R. Southon, R.C. Finkel, J. McAninch, Nucl. Instrum. Methods Phys. Res. B 258 (2007) 403–413.
[12] M. Martschini, P. Andersson, O. Forstner, R. Golser, D. Hanstorp, A.O. Lindahl, W. Kutschera, S. Pavetich, A. Priller, J. Rohlén, P. Steier, M. Suter, A. Wallner, Nucl. Instrum. Methods Phys. Res. B 294 (2013) 115–120.
[13] P. Sharma, P.W. Kubik, U. Fehn, H.E. Gove, K. Nishiizumi, D. Elmore, Nucl. Instrum. Methods Phys. Res. B 52 (1990) 410–415.
[14] D. Fink, A. Smith, Nucl. Instrum. Methods Phys. Res. B 259 (2007) 600–609.

Please cite this article in press as: K.M. Wilcken et al., Accelerator Mass Spectrometry on SIRIUS: New 6 MV spectrometer at ANSTO, Nucl. Instr. Meth. B (2017), http://dx.doi.org/10.1016/j.nimb.2017.01.003